Photoionization cross sections with excitation to $Ca^+ 3d$ and $4p$ levels

Zikri Altun and Hugh P. Kelly
Department of Physics, University of Virginia, Charlottesville, Virginia 22901
(Received 29 November 1984)

Photoionization cross sections of neutral calcium with excitation to Ca^+ $3d$ and $4p$ levels have been calculated from threshold to 50 eV by use of many-body perturbation theory. The cross section for leaving Ca^+ in the $4s$ ground level is also presented in this energy range and compared with the $3d$ and $4p$ cross sections which at their thresholds are larger than the $4s$ cross section. All three cross sections show interesting structure near 31 eV due to the $3p \rightarrow 3d$ resonance.

I. INTRODUCTION

In recent years there has been considerable interest in studying the satellite spectra of atoms,[1–10] which represent cross sections for photoionization with excitation. It is now many years since Wuilleumier and Krause[11] showed for Ne that such processes (including double photoionization) constitute approximately 20% of the total cross section over a wide range of energies.

Thus far, there have been relatively few calculations of cross sections for photoionization with excitation. There has been much recent interest for He leaving $He^+(n=2)$ and references to these calculations are given in the paper by Berrington *et al.*[12] Many-body perturbation theory (MBPT) has been used to calculate cross sections for photoionization of the neutral iron atom with excitation of a $4s$ electron to $3d$ or $4p$ levels.[13] Near threshold it was found that these processes were approximately 20% of the $4s \rightarrow \epsilon p$ cross section but were greater than the $4s \rightarrow \epsilon p$ cross section near 14 eV where the $4s \rightarrow \epsilon p$ cross section becomes small.[13] Ishihara *et al.*[14] have also used MBPT to calculate the cross section for photoionization of the $1s$ electron of neon accompanied by $2p \rightarrow 3s$ excitation. Recently Smid and Hansen[10] have calculated the ratio of the cross section for neutral argon leaving the ion in the $3p^4(^1D)nd$ levels to the cross section for $3s \rightarrow \epsilon p$ excitation.

For calcium, Altun[15] has calculated the cross sections for photoionization of Ca $(4s)^2$ leaving the ion Ca^+ $3d$ or $4p$ from threshold to 29 eV. In the threshold region for Ca^+ $3d$ (7.81 eV) and for $4p$ (9.25 eV) the $4s \rightarrow \epsilon p$ cross section passes through a minimum (at approximately 9 eV) and the $3d$ and $4p$ cross sections were found to be larger than the primary $4s \rightarrow \epsilon p$ cross section. Results have also been presented for the $4s \rightarrow \epsilon p$ cross section including single- and double-electron resonance structure.[16] A very interesting recent calculation by Scott, Kingston, and Hibbert[17] has used the R-matrix method[18] to calculate the photoionization cross section for neutral calcium from threshold at 6.11 eV to 9.25 eV, the threshold for Ca^+ $4p$. In this calculation the channels leading to Ca^+ $4s$, $3d$, and $4p$ are coupled to all orders. Scott *et al.*[17] have presented $4skp$, $3dkp$, and $3dkf$ cross sections between 7.9 and 9.0 eV. At the $3d$ threshold Scott *et al.*[17] have found that the $3d\epsilon p$ cross section is considerably larger than $4s\epsilon p$ or $3d\epsilon f$. They have also found large resonance structures in the dipole length approximation for all the partial cross sections between 7.9 and 9.0 eV due to $4pns$ and $4pnd$ double-electron resonances.

Cowan, Hansen, and Smid[19] have very recently calculated the cross section for neutral calcium between 11 and 28 eV leaving the Ca^+ ion in the $4s$, $3d$,and $4p$ levels. They have used the techniques described by Cowan.[20] They have also found that near threshold the Ca^+ $3d$ and $4p$ cross sections are larger than the Ca^+ $4s$ cross sections due to a minimum in the $Ca^+ 4s$ cross section.

In the present paper we extend the results of Altun[15] and present the results of our MBPT calculation for the $4s\epsilon p$, $3d\epsilon p$, $3d\epsilon f$, $4p\epsilon s$, and $4p\epsilon d$ cross sections for neutral calcium. Results are presented from the threshold for $3d$ (7.9 eV) to 50 eV. Particular attention is given to the region near 31 eV where there is a very large structure in each of the cross sections due to the $3p \rightarrow 3d$ resonance.

Section II contains an outline of the theoretical methods used. Section III contains the results of our calculations and comparison with other work, and Sec. IV contains our conclusions.

II. THEORY

In the calculations of this paper, we use the electric dipole approximation for absorption of electromagnetic radiation, and we neglect spin-orbit effects. Our Hamiltonian is

$$H = H_0 + H_c \ , \tag{1}$$

where

$$H_0 = \sum_{i=1}^{N} \left[-\tfrac{1}{2}\nabla_i^2 - Z/r_i + V(r_i) \right] , \tag{2}$$

and

$$H_c = \sum_{\substack{i,j=1 \\ i<j}}^{N} v_{ij} - \sum_{i=1}^{N} V(r_i) \ . \tag{3}$$

Atomic units are used throughout this paper. The term v_{ij} represents the Coulomb interaction between electrons i and j, and the single-particle potential $V(r_i)$ accounts for the average interaction of the ith electron with the remaining $N-1$ electrons.

In order to calculate photoionization cross sections, we require dipole matrix elements. The dipole length matrix elements are expressed as

$$Z_L(4s^2 \rightarrow nk) = \left\langle \psi_f \left| \sum_{i=1}^{N} z_i \right| \psi_0 \right\rangle , \tag{4}$$

where ψ_0 and ψ_f are exact many-particle ground and excited (continuum) states, respectively. The state ψ_f represents the excitation of $4s^2$ to nk, where n is a bound orbital and k is in the continuum. In our present calculations n is $4s$, $3d$, or $4p$.

The velocity form of the dipole matrix element is given by

$$Z_V(4s^2 \rightarrow nk) = \frac{1}{E_0 - E_f} \left\langle \psi_f \left| \sum_{i=1}^{N} \frac{d}{dz_i} \right| \psi_0 \right\rangle , \tag{5}$$

where E_0 and E_f are exact energy eigenvalues of H corresponding to ψ_0 and ψ_f. Since exact eigenstates ψ_0 and ψ_f are not known, we start from eigenstates of H_0 and use many-body perturbation theory[21-23] to develop a perturbation expansion in H_c for the states ψ_0 and ψ_f. Equivalently, we may write a perturbation expansion for the many-particle matrix elements Z_L or Z_V which contains one dipole interaction and any number of interactions with H_c. Diagrams contributing to Z_L are shown in Fig. 1, with exchange diagrams understood to be included. Time runs from bottom to top in the diagrams. Dipole matrix elements are represented by a solid dot and dashed lines represent correlation interactions with H_c. Coulomb interactions H_c below (above) the dipole interaction correspond to correlations in the ground (final) state.

In order to calculate the diagrams of Fig. 1 it is necessary to calculate a complete set of radial states for each value of orbital angular momentum which is used. These states satisfy the one-particle Schrödinger equation

$$\left[-\frac{\nabla^2}{2} - \frac{Z}{r} + V(r) \right] \phi_n = \epsilon_n \phi_n . \tag{6}$$

The general form of the potential for the single-particle states used in the evaluation of diagrams is[24]

$$V = R + (1-P)\Omega(1-P) , \tag{7}$$

where P is the projection operator given by

$$P = \sum_{n_{\text{occ}}} |n\rangle\langle n| , \tag{8}$$

where n_{occ} runs over occupied groundstate orbitals. In Eq. (7) R is the Hartree-Fock (HF) potential for ground-state orbitals, and Ω is a Hermitian operator chosen to give a physically appropriate potential for excited states.

The form of energy denominators occurring before the dipole interaction is

$$\sum_{j=1}^{N'} (\epsilon_{p_j} - \epsilon_{k_j}) , \tag{9}$$

and after the dipole interaction it is

$$\lim_{\eta \rightarrow 0^+} \sum_{j=1}^{N'} (\epsilon_{p_j} - \epsilon_{k_j}) + \omega + i\eta , \tag{10}$$

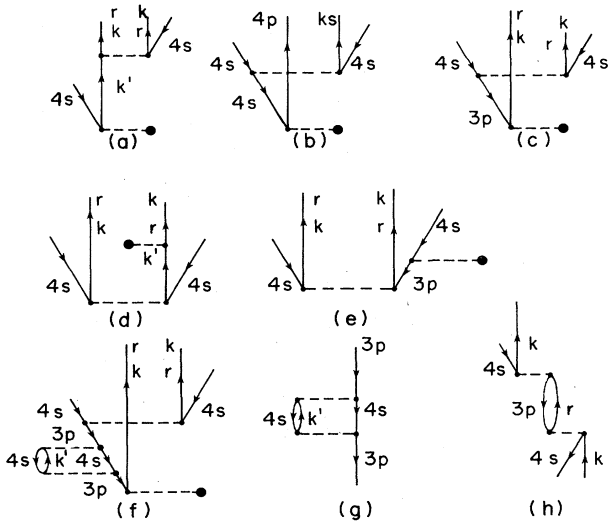

FIG. 1. Diagram and diagram segments contributing to the matrix element $Z(4s^2 \rightarrow r,k)$. Dashed line ending with isolated solid dot indicates matrix element of Z. Exchange diagrams are also included in the calculations. Diagram (f) represents Auger decay of $3p$ hole. (g) and (h) are segments of diagrams contributing to the width of the $3p \rightarrow 3d$ resonance.

where ϵ_{p_j} and ϵ_{k_j} are single-particle energies for a particle-hole pair and N' is the number of pairs excited. We also use

$$\lim_{\eta \rightarrow 0^+} (D + i\eta)^{-1} = PD^{-1} - i\pi\delta(D) , \tag{11}$$

where P represents principal-value integration. In calculating the sum over intermediate states k' in diagram 1(d) we used the differential-equation technique[25] which avoids taking dipole matrix elements between two continuum orbitals.

Radial $4p$ and $3d$ orbitals were calculated in the self-consistent HF approximation of excited ionic cores $3p^6 4p(^2P)$ and $3p^6 3d(^2D)$. The continuum ks and kd states were calculated in Hartree-Fock potentials appropriate to $3p^6 4pks,kd(^1P)$. Hartree-Fock potentials for kp and kf were derived from configurations $3p^6 3dkp,kf(^1P)$. In evaluating diagram 1(d), it was found to be important to use excited orbitals which have previously been found to give good account of energy correlations in second order.[16] When $r = 4p$, we calculated the ground-state correlation with $4p$ of $3p^6 4s\,4p(^1P)$ and $k'p$ of $3p^6 4sk'p(^1P)$. There is then an overlap factor between the final state $4p$ and the $4p$ of the ground-state correlation which is 0.812.

We also included effects of higher-order diagrams by using correlated dipole matrix elements involving $4s$ transitions in diagrams 1(a) and 1(b). The correlated dipole matrix elements were taken from the previous Ca $4s$ and $3p$ calculations by Altun *et al.*[16] Effects of the $3p \rightarrow 3d$ resonance were included by the geometric sum of segments shown in Fig. 1(h) with $r = 3d$.[16] In the present calculation we also included insertions of Auger-type on the $3p$ hole line as shown in Fig. 1(f). These may be summed geometrically by insertion of the segment shown in Fig. 1(g) into $3p$ energy denominators.

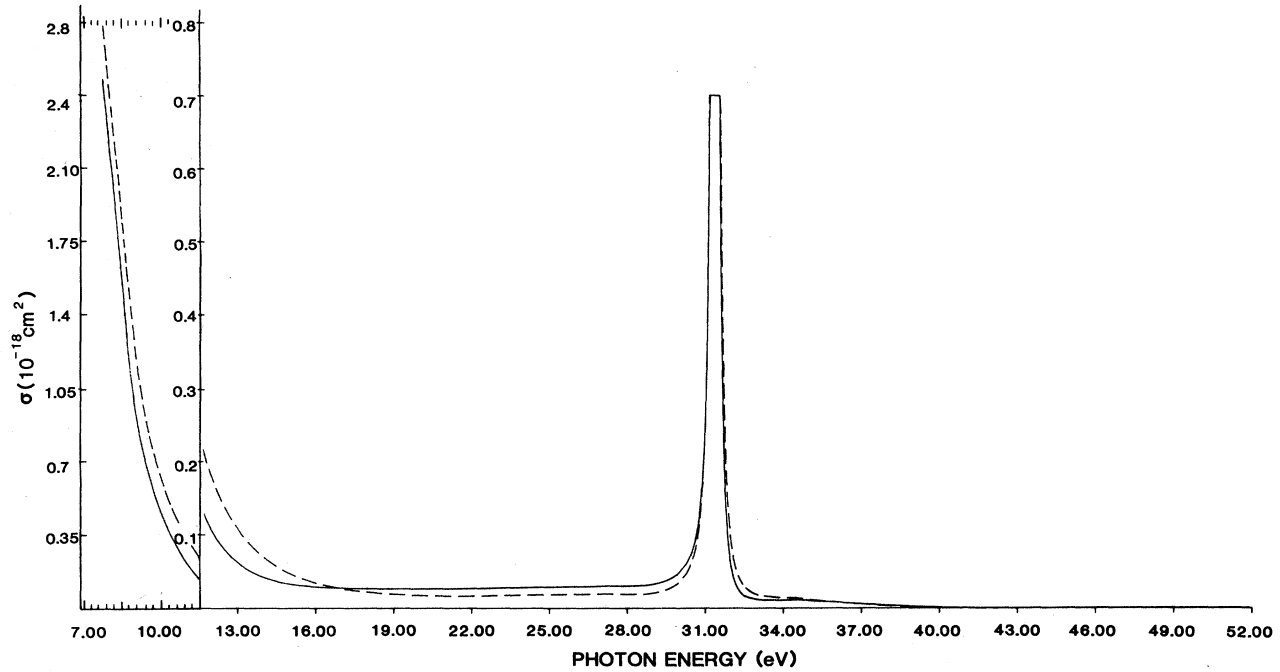

FIG. 2. Partial photoionization with excitation cross sections in dipole length (solid line) and dipole velocity (dashed line) formalism for $4s^2(^1S) \rightarrow 3dkp(^1P)$. The $3p \rightarrow 3d$ resonance at 31 eV peaks at 6.79 Mb (length) and 8.17 Mb (velocity).

III. RESULTS

In Fig. 2 we show our results for the $3dkp$ cross section in both dipole length and velocity approximations. We note the finite values at threshold followed by a rapid decrease, then almost constant values for 16 to 28 eV, and then the dramatic rise due to the $3p \rightarrow 3d$ resonance which peaks at 31.4 eV. If we had included spin-orbit splitting,

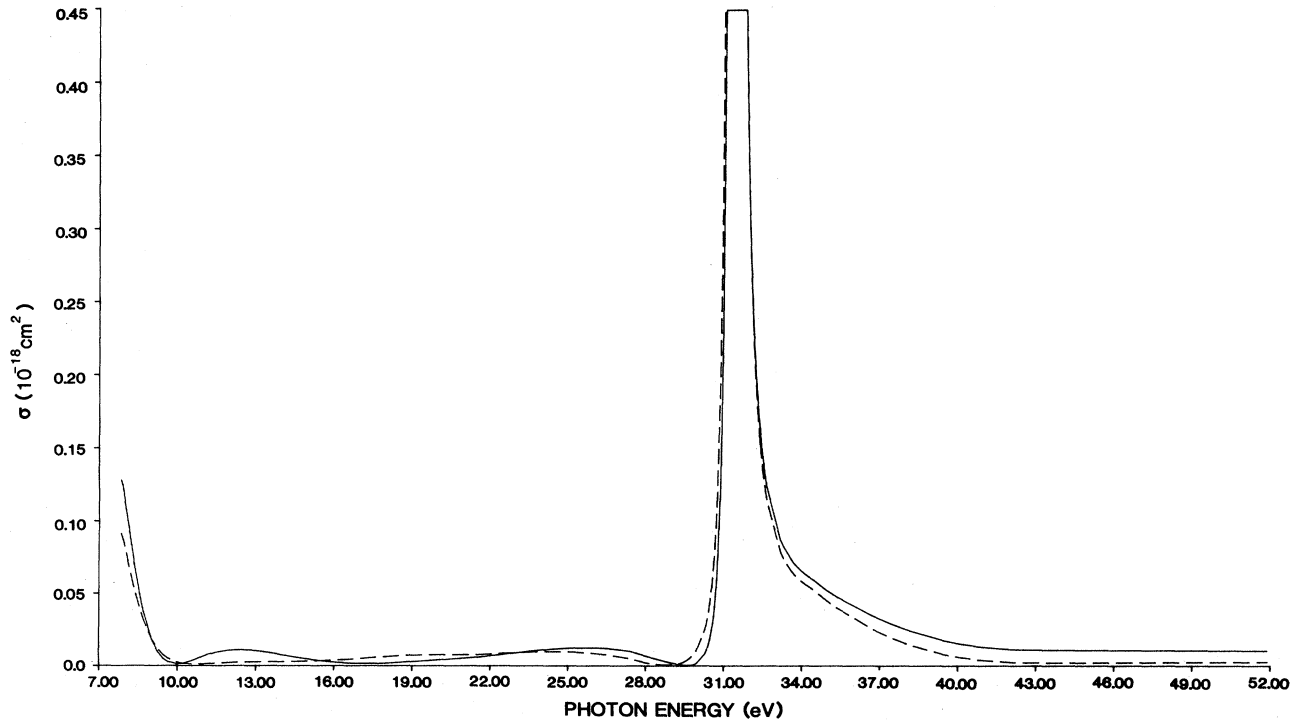

FIG. 3. Partial photoionization with excitation cross sections in dipole length (solid line) and dipole velocity (dashed line) formalism for $4s^2(^1S) \rightarrow 3dkf(^1P)$. The $3p \rightarrow 3d$ resonance peaks at 15.51 Mb (length) and 18.36 Mb (velocity).

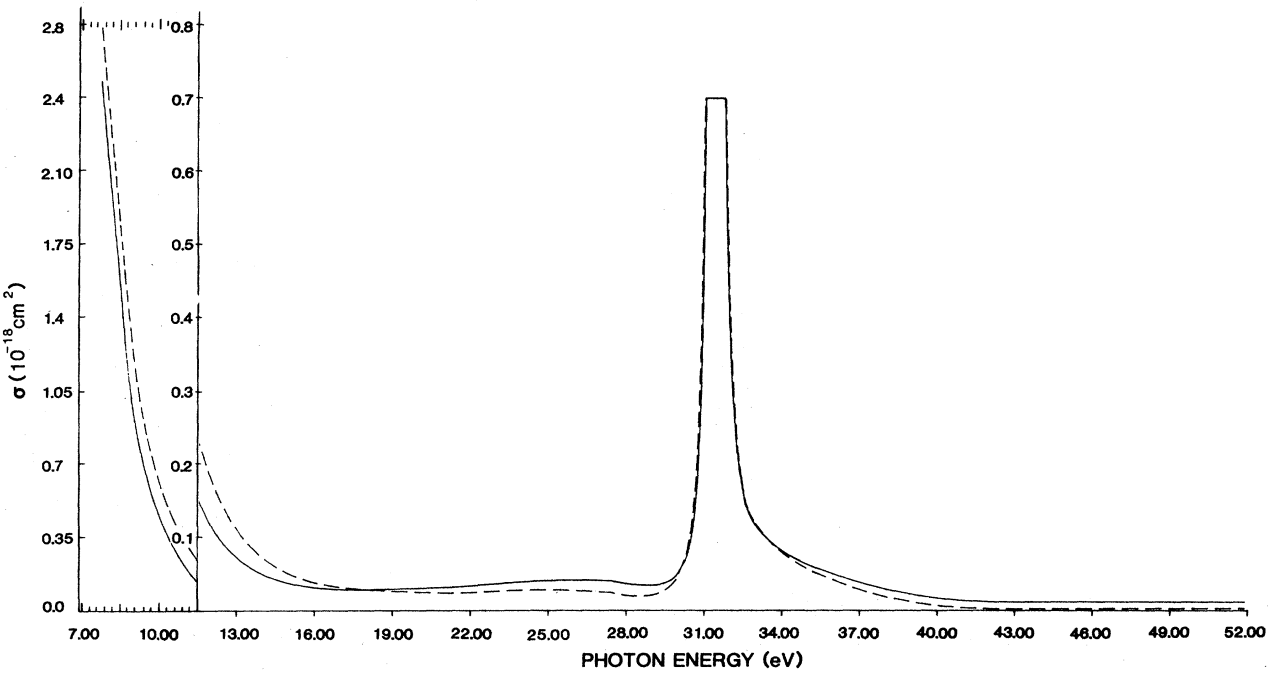

FIG. 4. Total $3d$ cross section. Solid line is dipole length calculation. Dashed line is dipole velocity calculation. This figure represents the sum of Figs. 2 and 3.

there would also be two narrower $3p \rightarrow 3d$ resonances (^3P at 24.81 eV and ^3D at 27.15 eV). For the length calculation there is considerable cancellation between final-state correlations of Fig. 1(a) and ground-state correlations of Fig. 1(d).

In Fig. 3 we present our results for the $3dkf$ length and velocity cross sections which are seen to be much smaller than the $3dkp$ cross sections. Near threshold the ratio of our $3dkf$ to $3dkp$ cross section is approximately 0.06, whereas it is approximately 0.28 for Scott *et al.*[17] We expect that the result of Scott *et al.* is the more accurate since they have coupled these and other channels, and the weak transition for $3dkp$ has borrowed strength from the stronger channels.

In both Figs. 2 and 3 we note the strong effects of the $3p \rightarrow 3d$ resonance. There is a very strong effect due to the diagram of Fig. 1(c) with $rk = 3dkp$ or $3dkf$. There is also an indirect contribution from the $3p \rightarrow 3d$ resonance from diagram 1(a) because the $4s \rightarrow kp$ transition also contains the $3p \rightarrow 3d$ resonance when higher-order terms are included. We note that the Fano[26] line profile does not go to zero, and this is attributed to the inclusion of the extra width due to the Auger-type process shown in Fig. 1(f). When only the width (decay) contribution of the segment of Fig. 1(h) is included, then the diagrammatic sums do correspond to the Fano theory.[26] In Figs. 2 and 3 our work also does not include the resonance structure near threshold due to double-electron $4pns$ and $4pnd$ excitations present in the length calculation by Scott *et al.*,[17] although not so clearly present in their velocity calculation. Our total $3d$ cross section for length and velocity is given in Fig. 4. The $3p \rightarrow 3d$ resonance in the $3dkp$ cross sec-

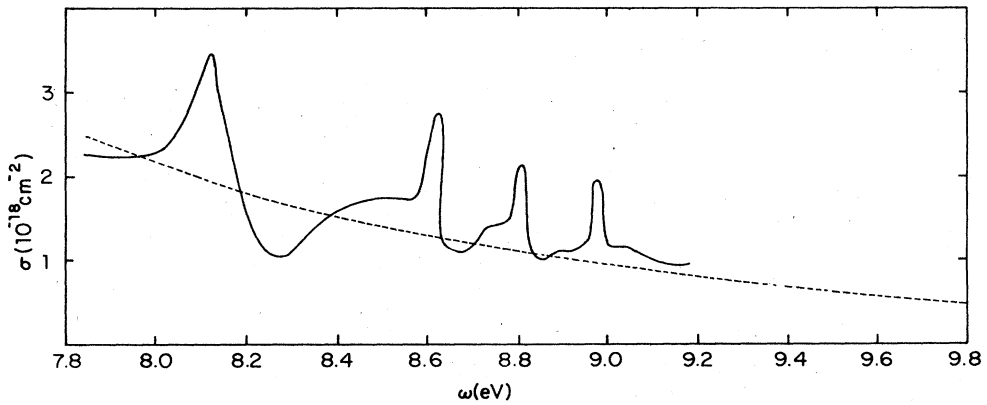

FIG. 5. Solid line represents total $3d$ cross section of Scott *et al.*, Ref. 17. Dashed line represents our MBPT length calculation.

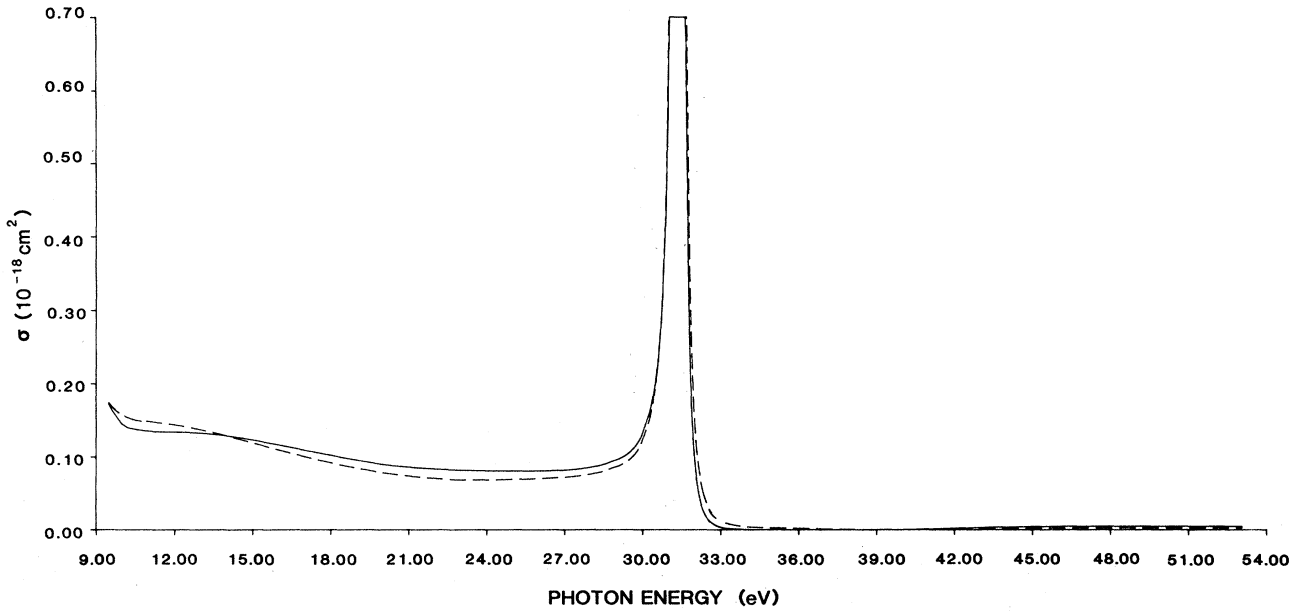

FIG. 6. Partial photoionization with excitation cross section for $4s^2(^1S) \rightarrow 4pks(^1P)$. Solid line is length formalism. Dashed line is velocity formalism. The $3p \rightarrow 3d$ resonance at 31 eV peaks at 13.1 Mb (length) and 15.6 Mb (velocity).

tions of Fig. 2 peaks at 6.79 Mb (length) and 8.17 (velocity). For the $3dkf$ cross section, the peaks are 15.51 Mb (length) and 18.36 Mb (velocity) (1 Mb$=10^{-18}$ cm^2). Between 12 and 20 eV we agree with Cowan *et al.*,[19] but beyond 20 eV their $3d$ cross section decreases.

In Fig. 5 our total $3d$ length cross section is compared with the $3d$ length cross section of Scott *et al.*[17] containing resonance structure. Their $3d$ velocity curve is approximately 60% higher than length at threshold and shows only weak resonance structure, unlike their length curve.

In Fig. 6 we present our $4pks$ cross section which starts at 0.17 Mb at threshold and decreases slowly until the effects of the $3p \rightarrow 3d$ resonance begin to dominate. It is interesting that the $3p \rightarrow 3d$ resonance is so strong since it is caused indirectly by the $3p \rightarrow 3d$ resonance in the $4s \rightarrow k'p$ channel which is coupled in Fig. 1(a) to the $4pks$ channel. The $3p \rightarrow 3d$ resonance at 31.4 eV peaks at 13.1 Mb (length) and 15.6 Mb (velocity). In these calculations there is much cancellation among the various diagrams, especially in the length case.

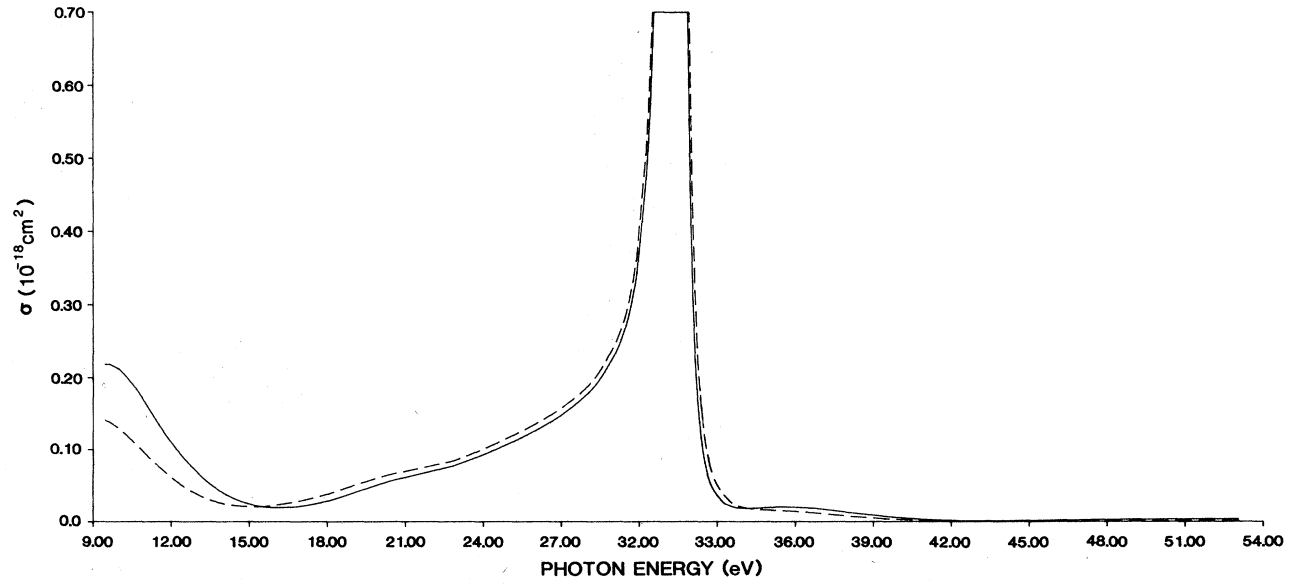

FIG. 7. Partial photoionization with excitation cross section for $4s^2(^1S) \rightarrow 4pkd(^1P)$. Solid line is length formalism. Dashed line is velocity formalism. The $3p \rightarrow 3d$ resonance at 31 eV peaks at 48.6 Mb (length) and 58.0 Mb (velocity).

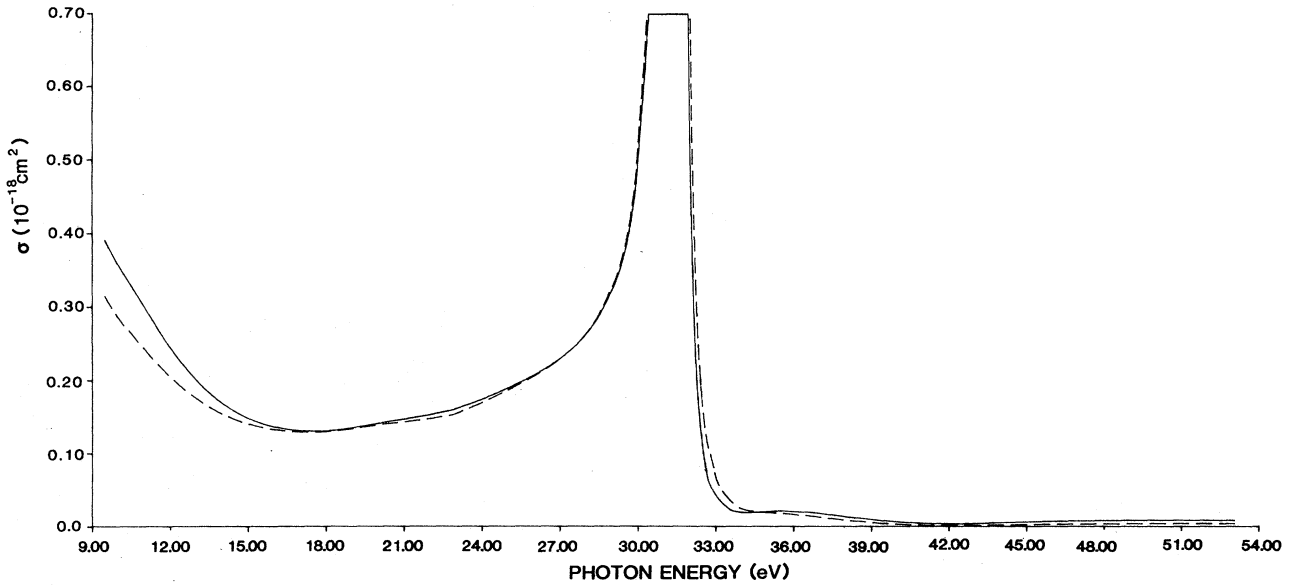

FIG. 8. Total $4p$ cross section. Solid line is length formalism. Dashed line is velocity formalism. The $3p \rightarrow 3d$ resonance at 31 eV peaks at 61.7 Mb (length) and 73.6 Mb (velocity).

In Fig. 7, we present our $4pkd$ cross section which again shows the large effect of the $3p \rightarrow 3d$ resonance in the $4s \rightarrow k'p$ channel. The $3p \rightarrow 3d$ resonance peak is 48.6 Mb (length) and 58.0 Mb (velocity). Again, there is much cancellation between final-state correlation and ground-state correlation. Figure 8 contains the total $4p$ cross section.

We have recalculated our previous $4skp$ cross section and omitted spin-orbit effects for comparison with our $3d$ and $4p$ cross section which were not calculated with spin-orbit effects. Our $4skp$ cross section σ_{4s} is shown in Fig. 9.

In Table I we present ratios for σ_{3d}/σ_{4s} and σ_{4p}/σ_{4s} length calculations at selected energy values. The corresponding velocity results are very close and are not presented.

We have also included the result obtained by Cowan *et al.*[19] at 21.2 eV, as well as the experimental value measured by Suzer *et al.*[7] We note that the measurements of

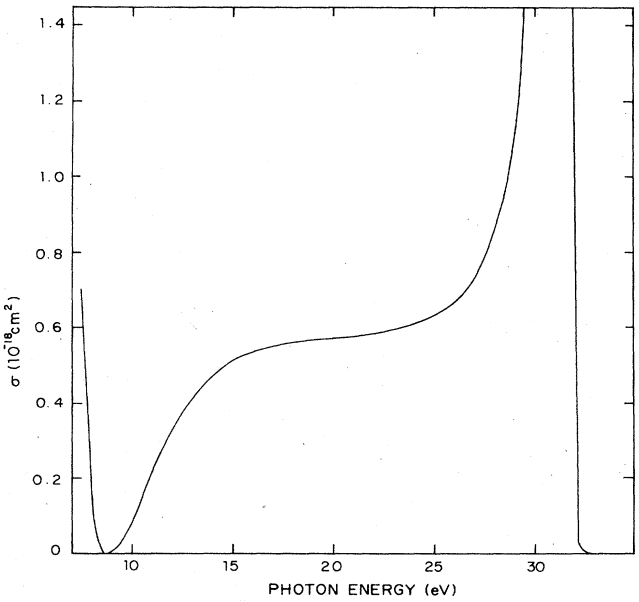

FIG. 9. Cross section for $4s^2 \rightarrow 4s\epsilon p(^1P)$. Spin-orbit effects are not included. Solid line is length formalism. Dashed line is velocity formalism. Double-electron resonances are not included in this cross section.

TABLE I. Cross-section ratios at selected energies for dipole length calculations.

Energy (eV)	σ_{3d}/σ_{4s}	σ_{4p}/σ_{4s}
12.8	0.1997	0.523
13.6	0.1263	0.396
14.8	0.0798	0.293
16.0	0.0597	0.252
17.4	0.052	0.234
19.8	0.0538	0.255
21.2	0.056	0.255
	0.04[a]	0.22[a]
	0.045[b]	0.103[b]
24.0	0.066	0.287
25.0	0.067	0.302
27.0	0.057	0.33
28.3	0.039 989	0.31
29.03	0.0277	0.286
30.6	0.0408	0.253
31.12	0.077 404 6	0.354

[a]Calculation by Cowan *et al.*, Ref. 19.
[b]Experiment by Süzer *et al.*, Ref. 7. Measurements taken at 90° and not adjusted for angular distribution.

Suzer *et al.* were taken at 90°, and a determination of the angular distributions for σ_{4p} and σ_{3d} are necessary for accurate comparison with experiment.

IV. DISCUSSION AND CONCLUSIONS

We have used many-body perturbation theory to calculate cross sections for photoionization for calcium leaving Ca^+ in the $3d$ and $4p$ levels. We have found that correlations both in the initial state and in the final state are very important and that there can be large cancellations between them. As a result, there is considerable uncertainty in the cross sections in such calculations. In all cases we have found good agreement between length and velocity calculations, but we are hesitant to conclude that this indicates the accuracy of the calculations. The calculations predict that near the minimum in the $4s\epsilon p$ cross section, the ratios σ_{3d}/σ_{4s} and σ_{4p}/σ_{4s} will exceed 1.00. This is particularly true for σ_{4p}/σ_{4s}. The calculations also predict very prominent resonance structure due to the $3p^5 4s^2 3d\,^1P$ resonance in $3d\epsilon l$, $4p\epsilon l$, and $4s\epsilon p$ cross sections. Although we are in reasonable agreement with Cowan *et al.*[19] for the $3d$ cross section and in agreement at 21.2 eV for the ratios of cross sections, our $4p\epsilon l$ and $4s\epsilon p$ cross sections differ considerably with those of Cowan *et al.*[19] It would be very desirable to have experimental partial cross sections or ratios of cross sections from the $3d$ threshold at 7.9 eV beyond the $3p \rightarrow 3d$ resonance at 31 eV.

It would also be very desirable to couple the different channels over a wide energy range, and we plan to do this with our coupled-equations method in the near future. It will be interesting to compare with Scott *et al.*[17] and we also expect resonance structure in the $4p$ cross section. Because of considerable cancellations among different diagrams and because there are many higher-order effects not included in this calculation, we cannot claim high accuracy for the calculation.

ACKNOWLEDGMENTS

We wish to thank the National Science Foundation for supporting this work. One of us (Z.A.) also thanks Marmara University of Istanbul, Turkey, for partial support. We thank the Computer Science Center of the University of Virginia for a computing grant. We are grateful to Dr. S. L. Carter and Dr. S. Salomonson for helpful discussions.

[1]F. J. Wuilleumier, *Atomic Physics,* edited by D. Kleppner and F. M. Pipkin (Plenum, New York, 1981), Vol. 7.
[2]M. O. Krause, in *Synchrotron Radiation,* edited by H. Winick and S. Doniach (Plenum, New York, 1980), p. 101.
[3]A. Fahlman, M. O. Krause, and T. A. Carlson, J. Phys. B **17**, 1217 (1984).
[4]H. Derenbach and V. Schmidt, J. Phys. B **17**, 83 (1984).
[5]R. D. Deslattes, R. E. LaVilla, P. L. Cowan, and A. Henins, Phys. Rev. A **27**, 923 (1983).
[6]P. H. Kobrin, S. Southworth, C. M. Truesdale, D. W. Lindle, U. Becker, and D. A. Shirley, Phys. Rev. A **29**, 194 (1984).
[7]S. Süzer, S.-T. Lee, and D. A. Shirley, Phys. Rev. A **13**, 1842 (1976).
[8]H. Schröder, B. Sonntag, H. Voss, and H. E. Wetzel, J. Phys. B **17**, 707 (1984).
[9]E. Schmidt, H. Schröder, B. Sonntag, H. Voss, and H. E. Wetzel (unpublished).
[10]H. Smid and J. E. Hansen, Phy. Rev. Lett. **52**, 2138 (1984).
[11]F. Wuilleumier and M. O. Krause, Phys. Rev. A **10**, 242 (1974).
[12]K. A. Berrington, P. G. Burke, W. C. Fon, and K. T. Taylor, J. Phys. B **15**, L603 (1982).
[13]H. P. Kelly, Phys. Rev. A **6**, 1048 (1972).
[14]T. Ishihara, J. Mizuno, and T. Watanabe, Phys. Rev. A **22**, 1552 (1980).
[15]Z. Altun, Ph.D. thesis, University of Virginia, 1982 (unpublished).
[16]Z. Altun, S. L. Carter, and H. P. Kelly, Phys. Rev. A **27**, 1943 (1983).
[17]P. Scott, A. E. Kingston, and A. Hibbert, J. Phys. B **16**, 3945 (1983).
[18]P. G. Burke and K. T. Taylor, J. Phys. B **8**, 2620 (1975).
[19]R. D. Cowan, J. E. Hansen, and H. Smid, Phys. Rev. A **31**, 2750 (1985).
[20]R. D. Cowan, *The Theory of Atomic Structure and Spectra* (University of California Press, Berkeley, 1981).
[21]K. A. Brueckner, Phys. Rev. **97**, 1353 (1955).
[22]J. Goldstone, Proc. R. Soc. London, Ser. A **239**, 267 (1957).
[23]H. P. Kelly, Adv. Theor. Phys. **2**, 75 (1968).
[24]L. M. Frantz, R. L. Mills, R. G. Newton, and A. M. Sessler, Phys. Rev. Lett. **1**, 340 (1958); B. A. Lippmann, M. H. Mittleman, and K. M. Watson, Phys. Rev. **116**, 920 (1959); R. T. Pu and E. S. Chang, *ibid.* **151**, 31 (1966); H. J. Silverstone and M. L. Yin, J. Chem. Phys. **49**, 2026 (1968); S. Huzinaga and C. Arnau, Phys. Rev. **84**, 244 (1951).
[25]R. M. Sternheimer, Phys. Rev. **84**, 244 (1951).
[26]U. Fano, Phys. Rev. **124**, 1866 (1961).